Hindawi
Mathematical Problems in Engineering
Volume 2020, Article ID 8149383, 13 pages
https://doi.org/10.1155/2020/8149383

Research Article

An Innovative Design of Decoupled Regenerative Braking System for Electric City Bus Based on Chinese Typical Urban Driving Cycle

Yanfeng Xiong, Qiang Yu, Shengyu Yan, and Xiaodong Liu

School of Automobile, Chang'an University, Xi'an 710064, Shanxi, China

Correspondence should be addressed to Yanfeng Xiong; xiongyanfeng118@126.com

Received 24 March 2020; Accepted 19 June 2020; Published 18 July 2020

Guest Editor: Sanghyuk Lee

This paper proposes a novel decoupled approach of a regenerative braking system for an electric city bus, aiming at improving the utilization of the kinetic energy for rear axle during a braking process. Three contributions are added to distinguish from the previous research. Firstly, an energy-flow model of the electric bus is established to identify the characteristic parameters which affect the energy-saving efficiency of the vehicle, while the key parameters (e.g., driving cycles and the recovery rate of braking energy) are also analyzed. Secondly, a decoupled braking energy recovery scheme together with the control strategy is developed based on the characteristics of the power assistance for electric city bus which equips an air braking system, as well as the regulatory requirements of ECE R13. At last, the energy consumption of the electric city bus is analyzed by both the simulation and vehicle tests, when the superimposed and the decoupled regenerative braking system are, respectively, employed for the vehicle. The simulation and actual road test results show that compared with the superposition braking system of the basic vehicle, the decoupled braking energy recovery system after the reform can improve the braking energy recovery rate and vehicle energy-saving degree. The decoupled energy recovery system scheme and control strategy proposed in this paper can be adopted by bus factories to reduce the energy consumption of pure-electric buses.

1. Introduction

Insufficient mileage has become the main obstacle that restricts the development of the pure-electric vehicle due to its layout, battery cost, energy density, and other restrictions, especially for an electric city bus. Under the premise of constant external constraints, improving the vehicle energy-saving efficiency is of great significance for extending the vehicle driving range [1–5]. There are many approaches to improve vehicle energy efficiency. This paper systematically analyzes the factors that affect vehicle energy efficiency and puts forward an engineering solution to improve energy efficiency, which is helpful to reduce the energy consumption of the vehicle.

1.1. Literature Review. Superposition type of braking energy recovery system is mainly used in an electric city bus, which applies motor braking synchronously on the original mechanical braking without changing the braking system of the original vehicle. For passenger vehicles, in addition to the superposition type, a decoupled braking energy recovery system is adopted for some models. Decoupled braking energy recovery products have been launched by Bosch, TRW, and other enterprises [6, 7]. At present, the researches on the braking energy of electric buses are comprehensive and in-depth. The main factors affecting braking energy recovery in pure-electric passenger vehicles were analyzed, which include braking strength, brake hydraulic cylinder pressure, and initial vehicle speed in literature [8]. The attachment coefficients of different road surfaces were analyzed, which would affect the braking energy recovery rate in the literature [9]. In literature [10], in addition to the braking energy recovery rate, two other braking energy recovery evaluation indicators were established, which are energy-saving contribution rate and driving range contribution rate. The former reflects the contribution of braking energy recovery to vehicle energy consumption, and the latter refers to

the increased driving range of vehicles with braking energy recovery function compared with the vehicles without this function. The definition of braking energy recovery contribution rate was proposed, which is the ratio of the recovered portion of the braking energy which can be converted into kinetic energy at the wheel end to the braking energy recovered by the whole driving condition in literature [11]. A specific test method for calculating the braking energy recovery rate was provided by literature [12], and the real-vehicle tests were carried out on three pure-electric vehicles. However, the relationship of the braking energy recovery rate vehicle driving range was not analyzed, which is analyzed quantitatively. Although the methods to improve the braking energy recovery rate were not mentioned in the literature [13, 14], predecessors have done a lot of useful exploration. The fuzzy rules for braking energy recovery based on practical and simulation experience were designed in the literature [15], without verified on a real vehicle. A fuzzy control strategy for braking energy recovery was proposed by the literature [16, 17], which aimed at small and medium braking strength. A decoupled braking energy recovery strategy for pure-electric passenger vehicles was proposed by literature [18]. VCU analyzed the driver's intention of the braking pedal and calculated the distribution of braking force between front and rear axles. The motor braking had the priority, and the insufficient part is provided by the hydraulic control unit. However, braking stability is not considered in this literature. Based on the known cycle condition, the model of braking prediction and distribution was developed in literature [19]. On the premise of braking stability, with the target of the maximum motor braking capacity and recovery efficiency, the model realized offline calculations in advance which met the real-time requirements of the table looking up online. Under the actual working condition, the robustness of the model still needs to be verified. A fuzzy control strategy for braking energy recovery was proposed, which took SOC and vehicle speed as input variables, and took a braking force of motor as output variables in literature [20]. It is helpful to recover more braking energy, but due to the unchanged braking system structure, the improvement is limited. The braking system structure was changed, in which the traditional hydraulic braking was replaced by EMB in literature [21]. Under the condition that ABS was not triggered and the braking strength was little, motor braking met the vehicle braking requirement. The validity of the strategy was verified in the HILLS environment, without verification for a real vehicle. A superposition braking energy recovery strategy for small pure-electric four-wheel-drive passenger vehicles was proposed in the literature [22]. Under small and medium braking strength, four motors recovered braking energy at the same time in order to increase the braking energy recovery rate. This power system configuration is less commonly used in pure-electric city buses. A braking energy recovery system scheme was proposed in literature [23], based on composite power supply combining power battery with supercapacitor. This scheme improves the capacity of braking energy recovery under large braking strength, but it is not applicable for an urban condition which is mainly small braking strength. Literature [24] optimized vehicle speed fluctuations to reduce energy consumption based on adaptive cruise function for pure-electric passenger vehicles. However, it is not applicable to frequent acceleration and deceleration conditions of urban buses. Pure-electric buses mainly operate on urban roads, and the small-strength braking condition is more than passenger vehicles. It is beneficial for improving the braking energy recovery rate of a pure-electric city bus by realizing motor braking in advance based on the control strategy of decoupled braking energy recovery. In addition, a pure-electric city bus is rear-motor rear-wheel-drive configuration with a large load of the rear axle, so the improvement of energy consumption on the braking-decoupled rear axle is better than that of the braking-decoupled front axle.

1.2. Motivation and Innovation. Pure-electric city bus driving form is basically rear-motor rear-wheel-drive configuration. Aiming at the energy dissipation path, the factors affecting vehicle energy-saving rate and braking energy recovery rate are hackled. In addition to constants such as transmission system and powertrain efficiency, the variables are mainly the ratio of motor braking force to mechanical braking force. Considering that the motor only acts on the rear axle which has a large load, it is helpful for increasing vehicle energy-saving rate and braking energy recovery rate by reducing mechanical braking force and action time on the rear axle. In order to realize the reduction just mentioned, a relief valve is increased on the braking gas road of the rear axle. Considering that axle-load distribution of small braking strength is not required in ECE braking regulations when the braking strength is small, the relief valve is closed and the rear axle is only under motor-braking, and when the braking strength is large, the relief valve is opened, and the rear axle is only under mechanical braking. This innovation is applicable for frequent small braking strength conditions of a city bus. Compared with the vehicle with the scheme and control strategy of this paper to superposition braking energy recovery scheme, the energy consumption is reduced by 3–7%, and the larger the rear axle loads, the more energy consumption decreases. It is proved to be feasible and effective by performance simulation and real-car verification. The new parts selected in this scheme are all mature, which are convenient for engineering.

1.3. Organization of the Paper. The remainder of the paper is organized as follows. Section 2 analyzes the influence factors of the energy-saving effect for the electric city bus. The scheme and control strategy of the decoupled braking energy recovery system is proposed in Section 3. The experimental verification of the decoupled braking system solution and the results discussion is implemented in Section 4, followed by the conclusions in Section 5.

2. Factors Affecting Vehicle Energy Conservation Effect

2.1. Vehicle Energy Dissipation Path. Considering working conditions, cost, and other factors, the driving configuration of a single motor and rear-motor rear-wheel-drive configuration is adopted by the electric city bus. Because the motor only acts on the rear axle, front axle braking can only be

completed by mechanical braking. The energy dissipation path is shown in Figure 1.

According to Figure 1, vehicle energy dissipation path is divided into three parts:

Part 1: Rear-wheel, half shaft, drive reducer, and transmission shaft. In this stage, the energy is transmitted in mechanical form.

Part 2: Motor and inverter. In this stage, the energy is transmitted in electrical form.

Part 3: Battery. In this stage, the energy is stored in chemical form.

When the vehicle is driven, battery-electric quantity E_B passes through the electric driving system, transmission shaft, and rear axle, and finally outputs driving energy E_T. The driving energy E_T needs to overcome driving resistance of the whole vehicle and then converts into mechanical energy. The mechanical energy of the front axle cannot be recovered, usually, that of the rear axle cannot be recovered totally. Braking energy recovery rate λ is defined as the ratio of motor recoverable energy E_{gen} to a total consumption of brake without the function of braking energy recovery E_T. Therefore, the recoverable energy at the position of the flange where the rear axle and the transmission shaft are connected is $\lambda E_T \eta_{tra}$, and the energy finally stored in the battery is E_B'. In the driving process, the output energy of transmission shaft is E_D, the output energy of the motor is E_{TM}, and that of battery is E_{dchg}; in the braking process, the output energy of transmission shaft is E_D', the recovered energy of the motor is E_{gen}, the recovered energy of the battery is E_{chg}, the mechanical efficiency of transmission shaft is η_{drv}, the mechanical efficiency of the rear axle is η_{tra}, the driving efficiency of the motor is η_{TM}, the recovery efficiency of the motor is η_{gen}, the discharging efficiency of the battery is η_{dchg}, and the recovery efficiency of the battery is η_{chg}. The vehicle energy flow distribution is shown in Figure 2.

As shown in Figure 2, the driving process energy consumption E_B is shown in

$$E_B = \frac{E_T}{\eta_{dchg}\eta_{TM}\eta_{dr\,v}\eta_{tra}}. \tag{1}$$

Energy recovery during braking is shown in

$$E_B' = \lambda E_T \eta_{tra}\eta_{drv}\eta_{gen}\eta_{chg}. \tag{2}$$

In order to analyze the vehicle energy-saving potential, the energy-saving degree of the whole vehicle η_{reg} refers to the ratio of the effective electric quantity recovered by braking to the electric quantity consumed by the whole vehicle without the function of braking energy recovery, which is shown in.

$$\eta_{reg} = \frac{E_B'}{E_B} = \lambda \cdot \eta_{gen}\eta_{TM}\eta_{chg}\eta_{dchg}\eta_{drv}^2\eta_{tra}^2. \tag{3}$$

The more energy-saving the degree of the whole vehicle is, the more energy can be reused. From (3), it can be seen that the vehicle energy-saving degree η_{reg} is related to driving efficiency η_{TM} and feedback efficiency η_{gen} of the motor system, discharge efficiency η_{dchg} and feedback efficiency η_{chg} of the battery system, efficiency η_{drv} of the transmission shaft, and mechanical efficiency η_{tra} of the rear axle and other constants and is directly proportional to the recovery rate of the braking energy λ.

The force analysis of the vehicle braking process is shown in Figure 3. In this figure, the normal reaction of the front axle is F_{zf}, the normal reaction of the rear axle is F_{zr}, the height of the vehicle mass center is h_g, the distance from the mass center to the front axle is a, the distance from the mass center to the rear axle is b, the load transfer of the front and rear axle during braking is G_z, the vehicle gravity is G, and the distance between the front and rear axle is L.

Combined with Figures 2 and 3, the braking energy recovery rate λ is shown in

$$\lambda = \frac{E_{gen}}{E_T} = \frac{\int P_{reg}\mathrm{d}t}{\int \left(P_{reg} + P_{hyd}\right)\mathrm{d}t} = \frac{F_{reg}}{F_{reg} + F_{xbf} + F_{xbr}}. \tag{4}$$

In (4), P_{reg} and F_{reg} refer to the braking power and force of the motor acting on the rear axle, respectively. P_{hvd} refers to the force of the mechanical braking system acting on the whole vehicle, consisting of F_{xbf} and F_{xbr}. The front axle braking force of the electric city bus is mechanical braking, so increasing the motor power P_{reg} and reducing the mechanical braking force of the rear axle F_{xbr} is beneficial to improving the braking energy recovery rate λ. The braking force of the whole vehicle, including F_{reg} and P_{hvd}, is strongly related to the driver's braking intention. The driver's braking intention refers to the driver's expectation of deceleration $\mathrm{d}v/\mathrm{d}t$ at current speed v, while the speed v and deceleration parameters $\mathrm{d}v/\mathrm{d}t$ are strongly related to the driving conditions of the vehicle, furthermore affecting the braking energy recovery rate λ.

2.2. Condition Parameters Analysis. The driving condition represents the speed-time of a vehicle in a certain area. There are many characteristic parameters in a driving condition, among which the speed parameters have a great impact on energy consumption [25]. Speed is mainly affected by morning and evening peak periods, road conditions, driving habits and other factors [26–29]. The ideal vehicle development model is to generate typical conditions by collecting the actual road conditions and carry out development verification based on typical conditions. However, considering the progress of the development and regulatory requirements, the test condition is always employed for actual vehicle development, while some actual conditions are also supplemented as reference.

There are two kinds of test conditions for city buses in China now: WTVC urban condition and CTUDC condition. The latter comes from China's automobile industry-standard named QC/T 759 "Urban Operation Cycle for Automobile test." The parameters of the actual conditions for Changchun, Jinan, Hangzhou, Dalian, and other typical

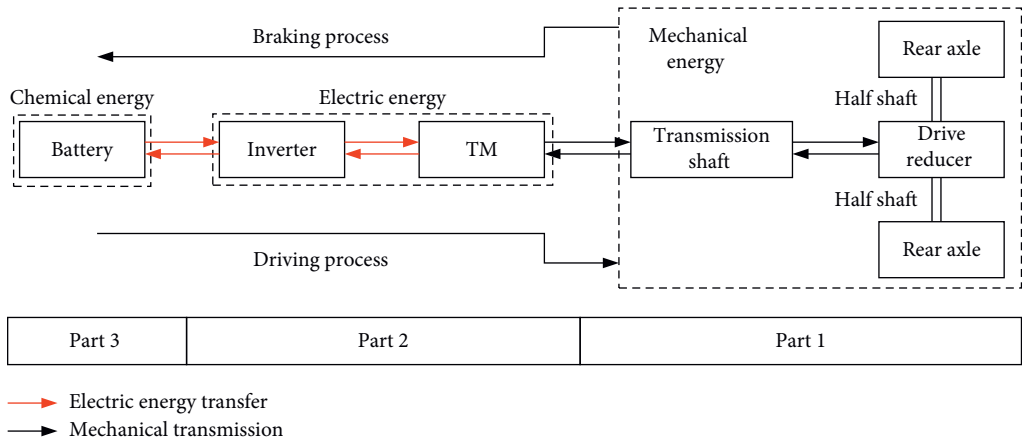

Figure 1: Vehicle energy dissipation path.

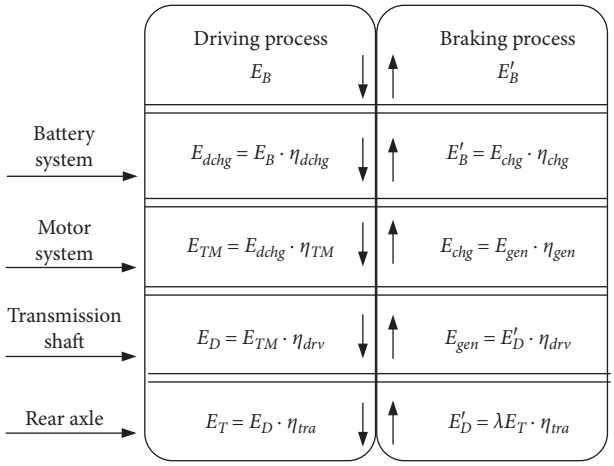

Figure 2: Vehicle energy flow distribution.

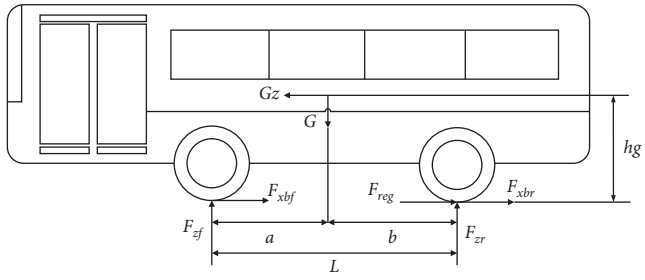

Figure 3: Analysis of the braking process of the vehicle.

cities in China are contrasted with the WTVC and CTUDC test conditions. The comparison results are shown in Table 1.

As is shown in Table 1, compared with the condition of WTVC, the characteristic parameters of CTUDC conditions are closer to the four actual typical cities in China, such as speed, proportion, acceleration, and other parameters. Due to the fact that CTUDC driving condition is more representative, it is adopted in this paper. The electric city bus studied in this paper is driven by a single motor, so the motor needs to meet the torque and power requirements when the whole vehicle is driven and braked. The distribution of speed and acceleration frequency based on CTUDC driving condition is shown in Figures 4 and 5.

As is shown in Figures 4 and 5, the low-speed part of 0~20 km/h accounts for 58.58% and the medium speed part of 20~40 km/h accounts for 35.44%, which means the vehicle speed mainly concentrate on medium and low speed. The acceleration reflects the driver's intention to change the speed. Considering the security of the standing passengers, the deceleration of the city bus is small. The maximum deceleration is 1.05 m/s^2, and the braking condition accounts for 26.57%. The condition features mentioned above are the data basis of the research on braking energy recovery in this paper. Whether the motor torque can cover the braking demand of the whole vehicle is the premise of realizing the braking energy recovery function. The frequency distribution of the vehicle braking torque demand under different vehicle speeds is shown in Figure 6.

As is shown in Figure 6, the average driving torque demand in the driving process is 1390 Nm, and the working time exceeding 2850 Nm accounts for 2.92% of the total driving condition. The peak torque of the motor which is 2850 Nm meets the vehicle driving demand under most of the driving conditions. During the braking process, the average braking torque demand is −2030 Nm, and the working time when the braking torque demand exceeds 2850 Nm accounts for 5.82%. The cost of the motor is directly proportional to the motor torque, and the whole vehicle does not recover part of the energy exceeding the motor peak torque.

2.3. Braking Regulations. In the process of braking energy recovery, the rear axle increases the motor braking force, which changes the braking force distribution between the front and rear axles. To change the threshold value, the ECE R13 braking regulations must be followed to ensure braking safety. For the double-axle bus, braking regulation is stipulated in ECE R13 that when the braking strength is less than 0.15 g, there is no requirement for the distribution of front and rear axle load. As is shown in Table 1, it can be seen that the braking strength of the city bus is less than 0.15 g no matter for the test or the actual conditions. In this case, the

Table 1: Characteristic parameters of typical driving conditions.

Name	Parameter	CTUDC	WTVC urban	Changchun	Jinan	Hangzhou	Dalian
Velocity class	Maximum speed (km/h)	60.00	66.20	50.50	39.00	47.80	50.20
	Average speed (km/h)	15.89	22.92	11.50	13.28	13.31	12.95
Proportion class	Idle time ratio (%)	29.00	16.70	16.79	34.43	32.71	29.3
	Constant speed time ratio (%)	8.70	24.60	1.64	2.36	2.85	1.63
Acceleration class	Maximum deceleration (m/s^2)	−1.05	−1.03	−0.77	−1.4	−1.21	−1.2

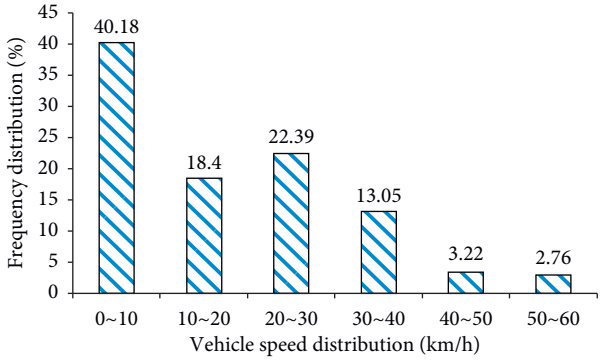

Figure 4: Vehicle speed frequency distribution of CTUDC.

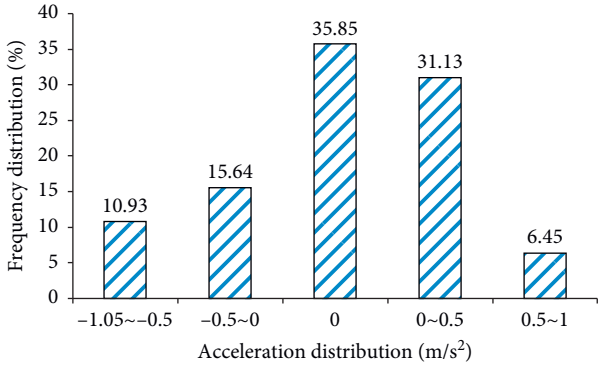

Figure 5: Acceleration frequency distribution of CTUDC.

regulation has no restriction on the distribution of braking force between two axles. Braking force distribution coefficient β is introduced as shown in

$$\beta = \frac{F_{xbf}}{F_{reg} + F_{xbf} + F_{xbr}} = 1 - \lambda - \frac{F_{xbr}}{F_{reg} + F_{xbf} + F_{xbr}}. \quad (5)$$

As is shown in Figure 3, the front axle load increases due to the forward movement of axle load during braking, and β increases accordingly. In order to improve the braking energy recovery rate, the rear axle braking force F_{xbr} should be reduced as much as possible. The superposition braking energy recovery scheme does not change the original vehicle braking system, which means mechanical and electric braking act at the same time, so the braking energy recovery has a common effect. In the decoupled scheme, electric braking takes priority, which can reduce the mechanical braking force of the rear axle to zero, so the recovery effect is better than the former.

There is no requirement for β in the CTUDC condition of the electric city bus, which can meet the requirements of braking regulations. The actual braking force is the smaller of the whole vehicle braking force and the road braking force. Considering that urban road in China is mainly asphalt pavement, the adhesion coefficient of dry asphalt pavement is usually 0.85, and that of wet asphalt is 0.5 [30]. Therefore, the adhesion coefficient of the road surface can meet the demand for vehicle braking energy recovery. The decoupled braking energy recovery scheme of an electric city bus is developed focusing on the reduction of the braking force for the rear axle, which is the key point to improve the braking energy recovery rate.

3. Scheme and Control Strategy of the Decoupled Braking Energy Recovery System

3.1. Decoupled Braking Energy Recovery Scheme. The superposition type of braking energy recovery scheme of the electric city bus does not change the original braking system, and the electric brake is applied synchronously on the basis of the mechanical brake of the rear axle. The advantage is that it does not increase any cost, and the disadvantage is that if the motor brake force applied is little, the recovery will have a common effect. Moreover, when the force is large, the rear axle will be easy to be locked first; then the vehicle may side out, which will affect the braking safety. The decoupled scheme needs to change the original braking system, which means a driver's braking intention will be judged by VCU, and the priority of motor braking will be realized.

A 12-meter electric bus is investigated in this paper. The main parameters of the vehicle and key assembly are shown in Table 2.

As is shown in Table 2, the curb weight of the vehicle is large, and the proportion between the front and rear axle loads is close to 1 : 2, when the vehicle is fully loaded. Making full use of the rear axle braking energy will be beneficial to improving the braking energy recovery rate. Therefore, a decoupled braking energy recovery scheme for electric city buses is proposed as shown in Figure 7.

As is shown in Figure 7, a relief valve, a check valve, and an air pressure sensor are installed at the front relay valve of the rear braking circuit of the bus. The relief valve is used to cut off the rear braking pipeline when braking with little intensity (e.g., less than 0.15 g), so as to realize the independent brake of the rear axle motor. On the contrary, the relief valve is opened by the large air pressure when braking with large intensity, and the electric and mechanical brake of the rear axle will work simultaneously. The check valve is used to realize that the air returns to the rear brake and ensure the air pressure balance in the brake pipeline when the braking strength changes from large to little. The air

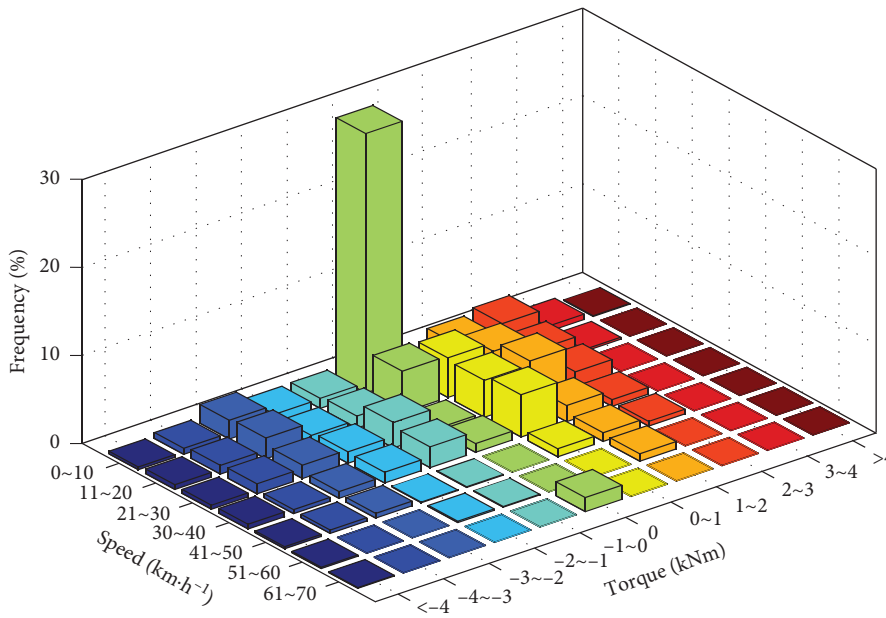

Figure 6: Frequency distribution of vehicle torque demand at different speeds.

Table 2: Main parameters of the vehicle key assembly.

Name	Parameters	Value
Vehicle	Wheel base (mm)	6100
	Distance between the centroid and front axle at curb/full weight (mm)	4095/3895
	Height of centroid at curb/full weight (mm)	758/1000
	Front and rear axle load at curb weight (kg)	4300/8800
	Front and rear axle load at full load (kg)	6500/11500
TM	Maximum torque (Nm)	2850
Battery	Capacity (Ah)	420
	Voltage (V)	384
	Maximum power (kW)	175
	Depth of discharge (%)	20~100
Transmission system	Drive shaft efficiency (%)	99
	Rear axle efficiency (%)	95

pressure sensor is used to identify the switch state of the relief valve and obtain the air pressure value of the rear brake chamber. The advantage of the scheme is that it does not change the distribution coefficient of the braking force and has good security. It is especially suitable for the little intensity braking condition of a city bus, which can ensure the priority of electric braking of the rear axle, thereby, improving the recovery rate of braking energy. Besides, it is easy to be realized in engineering with fewer mature parts be newly added; thus, it also has higher reliability and lower cost.

The whole vehicle is divided into two states during the braking process. (i) Based on the small braking strength: when the brake pedal is pressed, the front axle brake air chamber works normally while whether the rear axle brake air chamber works should be judged, owing to the fact that an overflow valve is equipped on the air pressure pipeline leading to the rear axle brake air chamber. If the air pressure of the pipeline is not enough to push the pressure limiting spring of the overflow valve, the rear axle brake air chamber will not enter the high-pressure gas. At this time, braking intention is identified by VCU through the brake pedal, and VCU judges whether the relief valve is open through a pressure sensor. According to the opening of the brake pedal and the air pressure difference between the front axle and the rear axle, VCU sends a request to the motor for the corresponding motor braking torque. (ii) Based on the large braking strength: in this case, the relief valve is open. VCU obtains the changes from the rear brake circuit, by a pressure sensor, stops motor braking, and recovers mechanical braking. At this time, the check valve is opened to realize the air pressure balance of the front and rear brake circuits.

3.2. Decoupled Braking Energy Recovery Strategy. The driver's braking intention is judged by VCU according to the brake pedal signal. Then, the braking torque of the motor acting on the rear axle is calculated by VCU in accordance with the ABS system, available battery power, vehicle speed, motor speed, and other information, while the front axle

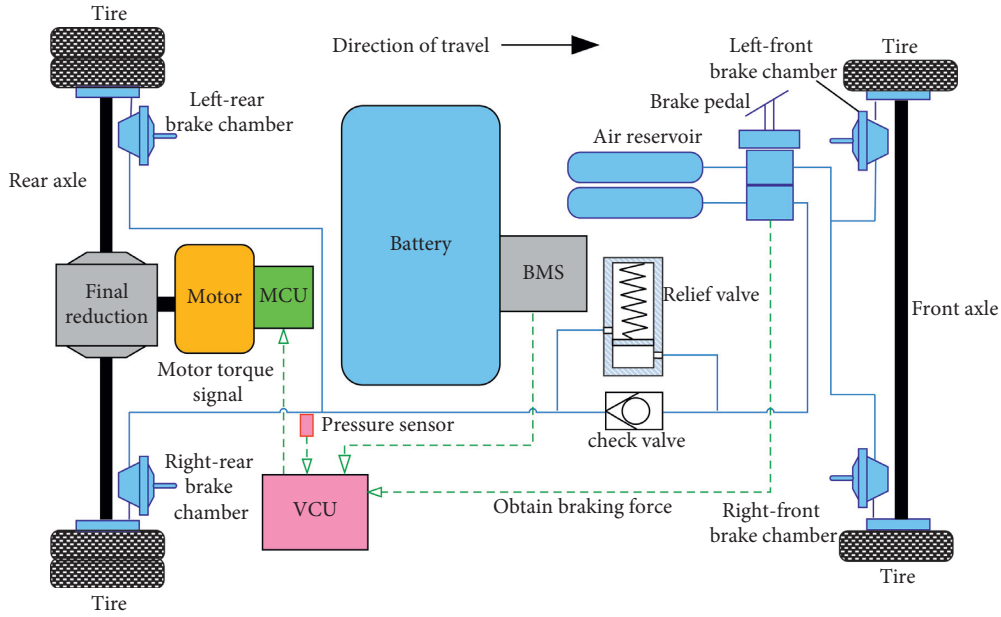

Figure 7: Decoupled braking energy recovery system for electric bus.

remains mechanical braking. The strategy is shown in Figure 8.

As is shown in Figure 8, the input signals of the braking energy recovery module include brake pedal opening signal, vehicle speed signal, ABS working signal, battery SOC, air pressure sensor signal, and the output signals including motor braking torque. The core of the algorithm is to compare the difference between rear axle braking torque demand and motor available torque. The strategy is shown in Figure 9.

As is shown in Figure 9, the driver's demand for braking force is reflected by the opening of the brake pedal. If the opening is confirmed, F_{br_req} will be confirmed accordingly. Air pressure of the brake wheel cylinder of the rear axle is represented by air pressure sensor through voltage value, and the actual air pressure value of the rear axle is uploaded to VCU. According to the conversion relationship between the air pressure of the rear axle and the mechanical braking torque, the actual mechanical braking torque of the rear axle F_{br_fric} can be obtained by the method of linear interpolation. The braking torque demand of the motor F_{reg_req} can be obtained by calculating the difference of the total braking torque of the rear axle F_{br_req} and the mechanical braking torque of the rear axle F_{br_fric}. The available torque of the motor F_{reg_act} is restricted by the output capacity of the motor and the feedback capacity of the battery. The former is mainly affected by the external characteristics and temperature of the motor, and the latter is mainly restricted by SOC and temperature of the battery cell. In order to ensure the battery life, its performance usually declines when SOC is high and the temperature is low. If the required braking torque of the motor F_{br_req} is higher than the available torque of the motor F_{reg_act}, it will be adopted as the required braking torque of the motor, and the insufficient part will be provided by the mechanical braking torque of the rear axle. If the required braking torque of the motor F_{br_req} is lower than the available torque of the motor F_{reg_act}, the required braking torque of the rear axle F_{br_req} will be provided totally by motor, and, at this time, the actual mechanical braking torque of the rear axle F_{br_fric} is zero, which is shown in

$$\begin{cases} \text{if } F_{br\_req} > F_{req\_act}; \quad sgn\left(F_{br\_fric}\right) = F_{br\_req} - F_{req\_act}, \\ \text{if } F_{br\_req} < F_{req\_act}; \quad sgn\left(F_{br\_fric}\right) = 0. \end{cases} \tag{6}$$

4. Results and Discussion

4.1. Simulation Verification. The main parameters of the whole vehicle and key assembly of electric bus studied in this paper are shown in Table 2, and the whole vehicle simulation model is built in AVL-CRUISE, as shown in Figure 10.

The map of motor efficiency used in the model is shown in Figure 11.

As is shown in Figure 11, during the driving process, the motor is in the high-efficiency area when the speed is 1000~1500 r/min (corresponding to the vehicle speed of 25~36 km/h) and the torque is 800–1500 Nm, which is basically consistent with the distribution of vehicle torque demand shown in Figure 6, and the driving efficiency of the motor is equivalent to the feedback efficiency. The battery system can be regarded as an equivalent circuit composed of open-circuit voltage and equivalent internal resistance in series [31]. The open-circuit voltage and equivalent internal resistance are functions of battery SOC, and the characteristics of the battery cells are shown in Figure 12.

As is shown in Figure 12, with the increase of SOC, the open-circuit voltage of the cell also becomes larger, and the internal resistance of the battery system is the same. When SOC is more than 20%, the internal resistance of the battery system is relatively small and stable. When SOC is less than

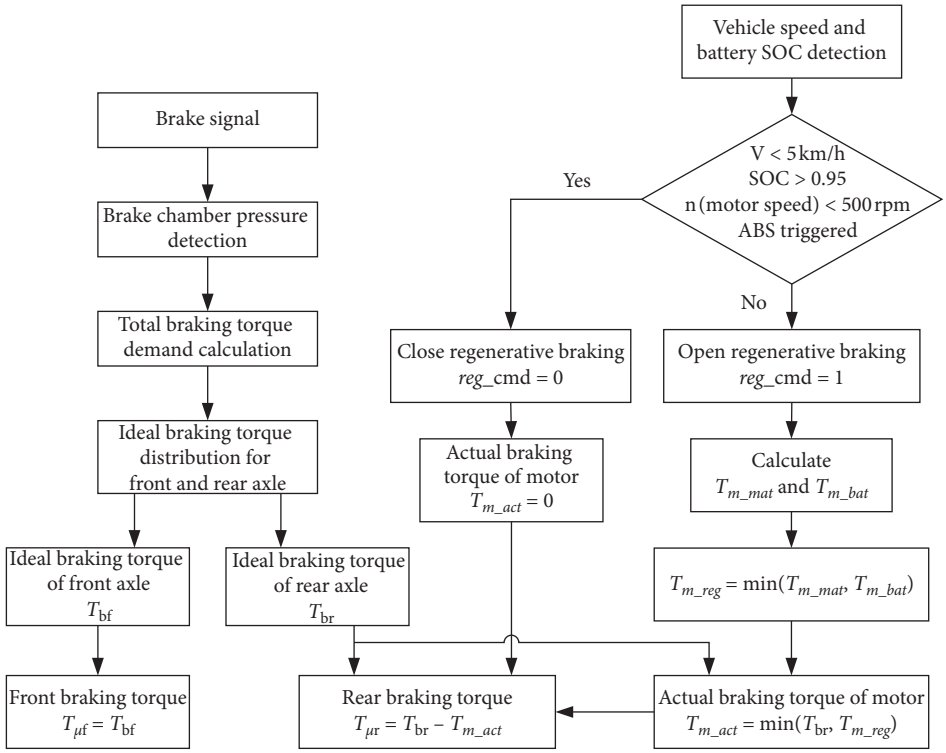

Figure 8: Decoupled braking energy recovery strategy flow chart.

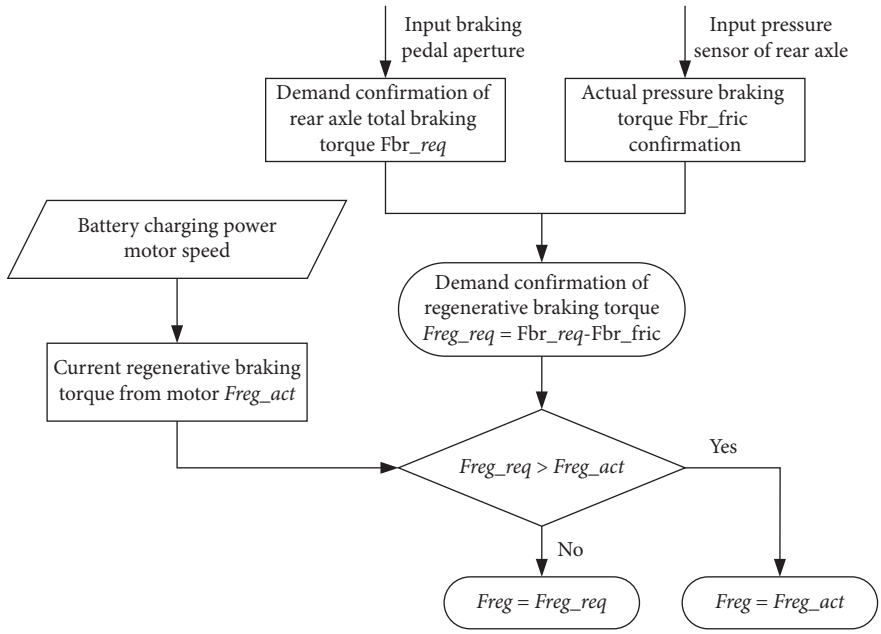

Figure 9: Decoupled control strategy of braking energy recovery.

20%, the internal resistance of the battery system increases sharply, corresponding to 80% of DOD as shown in Table 2. The decoupled braking energy recovery strategy is shown in Figures 9 and 10. The superposition braking energy recovery strategy calculates the braking torque of the motor based on the linear interpolation according to vehicle speed and brake pedal opening. Combined with the actual brake pedal opening which is usually 15~30% [32], the braking torque of the motor acting on the rear axle at different vehicle speeds is shown in Figure 13.

As is shown in Figure 13, when the vehicle speed is less than 10 km/h, the recoverable mechanical energy of the whole vehicle is small and the motor braking is not involved considering the vehicle braking smoothness. Under the same

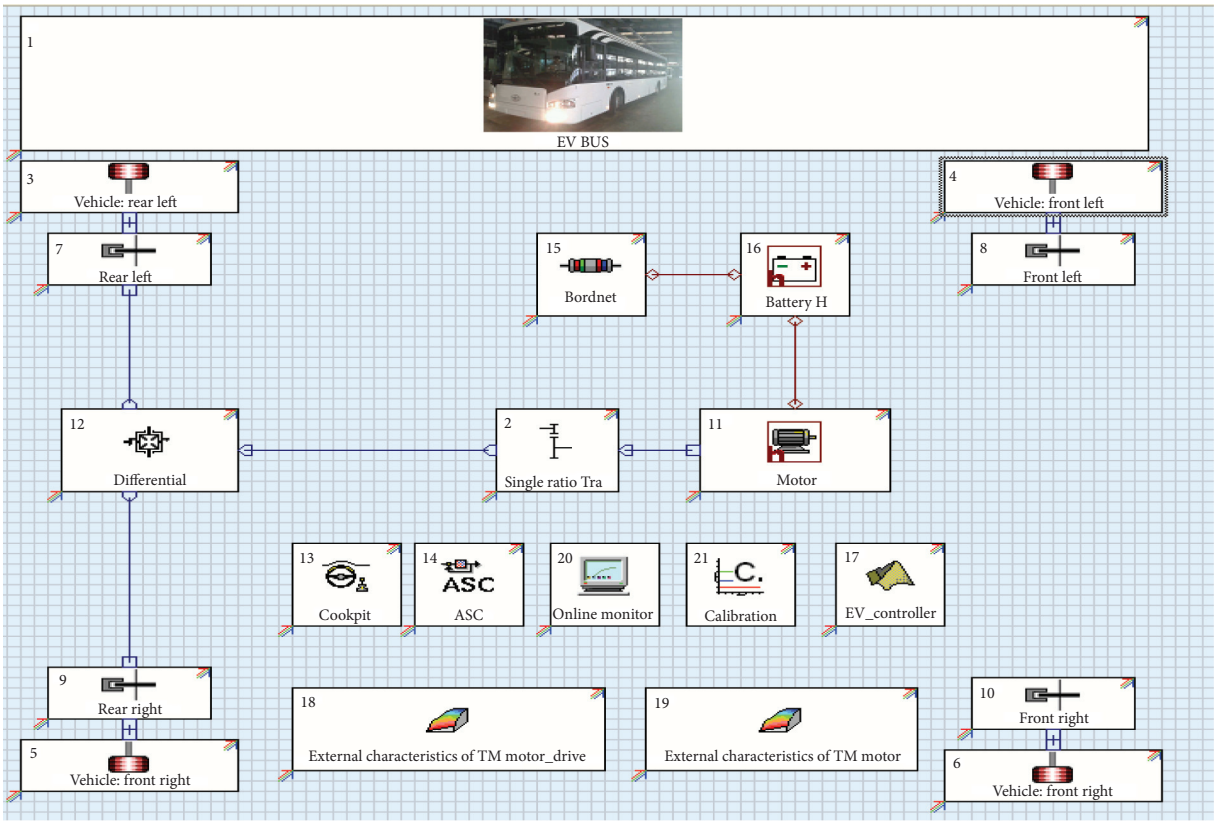

Figure 10: Physical model of performance simulation.

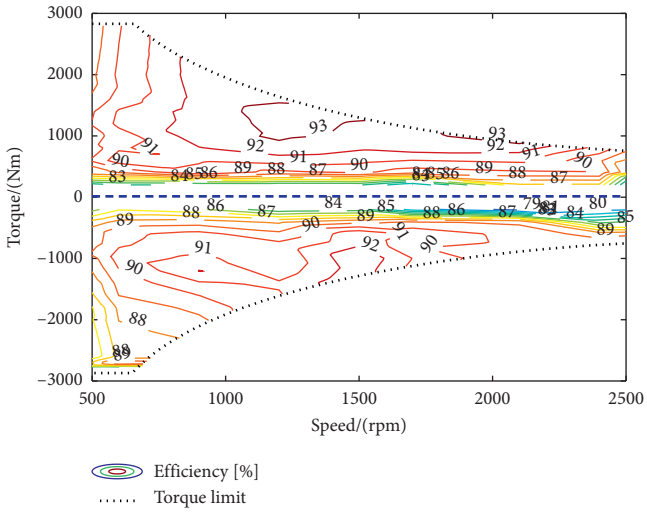

Figure 11: Motor efficiency MAP.

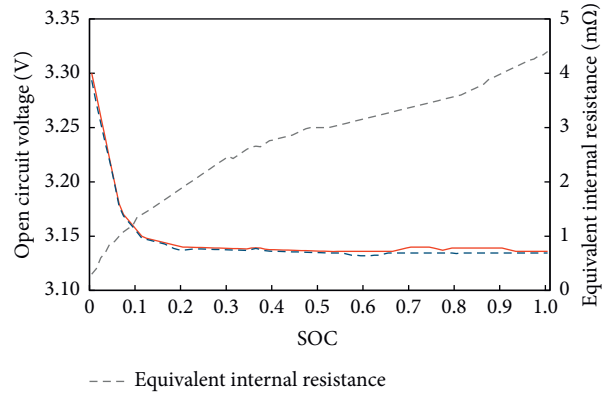

Figure 12: Changes of open-circuit voltage of the cell and internal resistance with SOC.

brake pedal opening, when the vehicle speed is in 10~55 km/h, the motor braking torque becomes larger correspondingly with the increase of the vehicle speed. When the vehicle speed is more than 55 km/h, the motor braking torque decreases correspondingly with the increase of the vehicle speed, mainly because the motor torque starts to decrease after the motor speed is higher than the base speed point. Based on CTUDC condition, vehicle energy consumption results of different loads under decoupled and superposition types of the braking energy recovery scheme are shown in Table 3.

As is shown in Table 3, as for the energy-saving effect compared with superposition type, the larger the vehicle curb weight is, the more significant the decoupling braking energy recovery scheme is. When the vehicle is fully loaded, there is 8.01% as power saving, while the half load and empty load, respectively, correspond to 5.17% and 3.01%. The main reasons are as follows. (i) The braking strength under CTUDC condition is small, and the motor peak torque

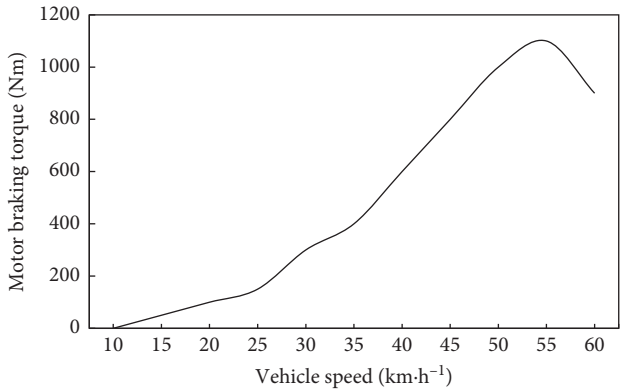

Figure 13: Braking torque of motor at different speeds.

Table 3: Vehicle energy consumption under different loads.

Load type	Simulation power consumption/(kWh/100 km)	
	Superimposing	Decoupling
Full load	93.6	86.1
Half load	79.3	75.2
Empty load	66.5	64.5

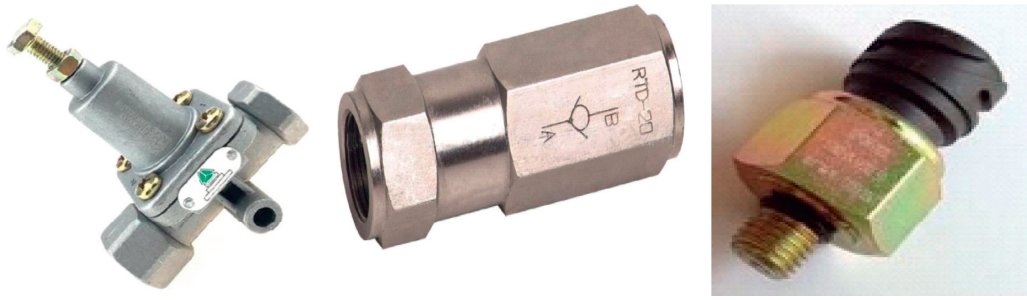

(a) (b) (c)

Figure 14: New parts. (a) Relief valve. (b) Check valve. (c) Air pressure valve.

covers the vehicle braking demand more than 95%. Compared with the superposition braking energy recovery scheme, the motor of the decoupled type can be more fully involved in the rear axle braking, while the mechanical braking of the rear axle is less involved. (ii) As is shown in Table 2, with the axle load change from zero to full, the rear axle load increases by 500 kg compared with the front axle load. The main reason is that except for sitting passengers, standing passengers are mainly concentrated in the wheelbase and the rear suspension. The rear axle load increases more than the front axle load, and the base of mechanical energy conversion at the rear axle is more than that with an empty load, so there is more braking energy that can be recovered.

4.2. Test Verification. The original electric bus adopts the superposition braking energy recovery scheme. Under CTUDC condition, it completes the energy consumption tests without braking energy recovery function and with superposition recovery function. After that, it is transformed into a sample vehicle with a decoupling braking energy recovery function. The restructuring scheme is shown in Figure 7, and the newly added parts are shown in Figure 14.

The actual road test was carried out in the test field of Tongliao, Jilin Province, China. The vehicle speed and mileage information were collected by VBox, and the driving data was collected by CANoe. CTUDC is adopted for the whole vehicle test condition, and the actual test speed follows the curve shown in Figure 15.

As is shown in Figure 15, the difference between the test speed and CTUDC condition speed is less than 2 km/h, which means the actual speed follows CTUDC well and the test data is valid. Statistics are made for the power consumption of the whole vehicle in three states: without braking energy recovery function, superposition, and decoupled braking energy recovery functions, respectively. The results are shown in Table 4.

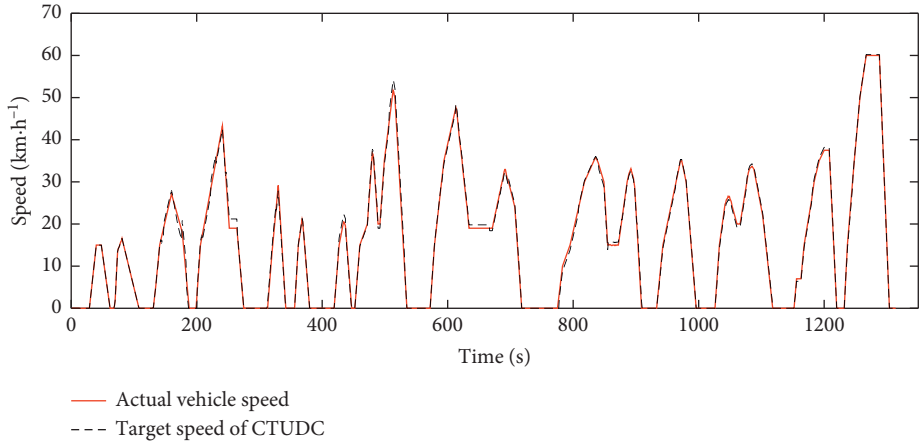

Figure 15: Test condition and actual speed.

Table 4: Test data under different braking energy recovery strategies.

Load type	Measured power consumption/(kWh/100 km)		
	Without braking energy recovery function	Superposing	Decoupling
Full load	122.14	89.28	82.97
Half load	110.04	81.36	76.09
Empty load	91.43	67.89	64.99

As is shown in Table 4, compared with the superposition braking energy recovery scheme, the decoupled one has 7.07% as energy-saving at full load and 6.48% and 4.27% at half load and empty load, respectively. The error between the measured results and the simulation results is within 1.5%, which verifies the feasibility and effectiveness of the scheme. Combined with Table 4 and (3), the energy-saving degree of the whole vehicle η_{reg} can be calculated. The energy-saving degree of the whole vehicle with the superposition braking energy recovery function is 26.91% at full load, 26.06% at half load, and 25.75% at empty load, and that with decoupled function is 32.07% at full load, 30.85% at half load, and 28.92% at empty load. Aiming at energy-saving degree, based on the same vehicle model, only under the premise of changing braking energy recovery function, compared with superposition type, the decoupled one energy-saving efficiency increases by 5.17% at full load, 4.79% at half load, and 3.17% at empty load. Under the load situation mentioned above, the energy-saving efficiency of the whole vehicle accounts for about 74% of the braking energy recovery rate. According to the energy-saving efficiency model of the whole vehicle, there are efficiency losses of the motor, battery, and transmission systems. The energy dissipation path is the same, so the overall efficiency loss is basically the same, which also verifies the effectiveness of the vehicle energy-saving model.

5. Conclusions

(1) Through identifying the energy dissipation path of the electric city bus, analyzing the whole vehicle force in the braking process, and establishing the whole vehicle energy-saving model, which contains the model constant of assembly efficiency, such as motor, battery, and transmission system, the whole vehicle energy-saving rate is proportional to the braking energy recovery rate, and the braking energy recovery rate is strongly related to the condition parameters such as speed and deceleration. Through analyzing the characteristic parameters of the urban condition and the single motor with rear-motor rear-wheel-drive configuration, it is concluded that reducing the mechanical braking force of the rear axle can effectively improve the recovery rate of braking energy.

(2) A decoupled braking energy recovery scheme and algorithm is proposed. In this scheme, relief valve, check valve, and air pressure sensor are added to the rear brake air circuit of the whole vehicle, so that the mechanical braking of the rear axle is not involved in the case of small braking intensity. The core of the algorithm is to get the actual mechanical braking torque of the rear axle according to the air pressure value of the rear brake air circuit and calculate the difference of total braking torque demand of the rear axle and the actual mechanical demand, compared with the available torque of the motor, and the ideal braking torque of the motor acting on the rear axle can be obtained. This scheme is particularly suitable for urban conditions, in which the newly added three parts are mature products with low cost and high reliability, which is conducive to engineering.

(3) Based on the scheme and algorithm mentioned above, the single factor energy consumption test is

carried out on the same vehicle. The road test results show that compared with superposition type, the decoupling type braking energy recovery rate is increased by 4~7% under different loads, and the energy-saving degree is increased by 3~5%, which verifies the feasibility and effectiveness of the scheme. The ratio of the test results of the whole vehicle energy-saving degree and the braking energy recovery rate both is 74%, which verifies the validity of the vehicle energy efficiency model.

(4) The decoupled braking energy recovery scheme proposed in this paper realizes the decoupled brake of the rear axle. In the next step, the front axle brake air circuit is to be modified in order to further improve the energy-saving rate and braking energy recovery rate and reduce the energy consumption of the whole vehicle. Meanwhile, braking smoothness of the decoupled scheme should be further researched.

Abbreviations

WTVC: World transient vehicle cycle
HAS: Hydraulic actuation system
DP: Dynamic programming
VCU: Vehicle control unit
TM: Traction motor
EMB: Electronic mechanical brake
DOD: Depth of discharge
SCB: Slip control boost
CTUDC: Chinese typical urban driving cycle
ECB: Electric city bus
SOC: State of charge
HILS: Hardware in the loop simulation.

Data Availability

The data used to support the findings of this study are available from the corresponding author upon request.

Conflicts of Interest

The authors declare that they have no conflicts of interest.

Acknowledgments

This work was supported by the Nature Science Foundation of China with Grant no. 51507013.

References

[1] M. Ehsani, Y. Gao, and A. Emadi, *Modern Electric,hybrid lectric and Fuel Cell Vehicles: Fundamentals, Theory, and Design*, CRC Press, New York, NY, USA, 2nd edition, 2009.

[2] S. Hano and M. Hakiai, "New challenges for brake and modulation systems in hybrid electric vehicles and electric vehicles," in *Proceedings of the 39th JSAE Conference*, Tokyo, Japan, May 2011.

[3] G. Sovran, "The impact of regenerative braking on the powertrain delivered energy required for vehicle propulsion," *SAE Paper*, vol. 12, no. 4, pp. 891–906, 2011.

[4] J. Tong and L. Zhang, "Analysis of domestic bus market performance of 2018 and outlook of 2019," *Commercial Vehicle*, vol. 38, no. 1, pp. 25–28, 2019.

[5] K. Nanda and C. Shankar, "Cooperative control of regenerative braking and friction braking for a hybrid electric vehicle," *Journal of Automobile Engineering*, vol. 230, no. 1, pp. 103–116, 2016.

[6] T. Okano, S. Sakai, and T. Uchida, "Braking performance improvement for hybrid electric vehicle based on electric motor's quick torque response," in *Proceedings of the 19th Electric Vehicle Symposium*, EVS, Pusan, Republic of Korea, October 2002.

[7] D. Kim and H. Kim, "Vehicle stability control with regenerative braking and electronic brake force distribution for a four-wheel drive hybrid electric vehicle," *Proceedings of the Institution of Mechanical Engineers, Part D: Journal of Automobile Engineering*, vol. 220, no. 6, pp. 683–693, 2006.

[8] Q. Guo, Z. Zhao, P. Shen, X. Zhan, and J. Li, "Adaptive optimal control based on driving style recognition for plug-in hybrid electric vehicle," *Energy*, vol. 186, no. 11, pp. 824–837, 2019.

[9] K. Itani, A. De Bernardinis, Z. Khatir, and A. Jammal, "Comparison between two braking control methods integrating energy recovery for a two-wheel front driven electric vehicle," *Energy Conversion and Management*, vol. 122, no. 8, pp. 330–343, 2016.

[10] L. Chu, D. Liu, H. Liu et al., "A Study on the evaluation method of braking energy recovery in battery electric vehicle," *Automotive Engineering*, vol. 39, no. 4, pp. 471–479, 2017.

[11] B. Qiu and Q. Chen, "Evaluation method of regenerative braking for electric city bus," *Journal of Mechanical Engineering*, vol. 48, no. 16, pp. 80–85, 2012.

[12] L. Chu, J. Cai, and Z. Fu, "Research on brake energy regeneration evaluation and test method of pure electric vehicle," *Journal of Hua Zhong University of Science and Technology*, vol. 42, no. 1, pp. 18–22, 2014.

[13] S. Gino, "The impact of regenerative braking on the powertrain-delivered energy required for vehicle propulsion: 2011-01-0891," in *Proceedings of the SAE 2011 World Congress & Exhibition*, Detroit, MI, USA, April 2011.

[14] S. Pan, Z. Song, and X. Wang, "Control strategy for electromechanical braking of electric vehicle," *Control Engineering of China*, vol. 24, no. 2, pp. 309–314, 2017.

[15] Y. F. Xin, T. Z. Zhang, H. G. Zhang, Q. Zhao, J. Zheng, and C. Wang, "Fuzzy logic optimization of composite brake control strategy for load-isolated electric bus," *Mathematical Problems in Engineering*, vol. 2019, Article ID 9735368, 14 pages, 2019.

[16] S. Q Li, B Yu, and X. Y Feng, "Research on braking energy recovery strategy of electric vehicle based on ECE regulation and I curve," *Science Progress*, vol. 17, no. 1, pp. 762–779, 2019.

[17] D. Zhao, L. Chu, N. Xu, C. Sun, and Y. Xu, "Development of a cooperative braking system for front-wheel drive electric vehicles," *Energies*, vol. 11, no. 2, pp. 377–401, 2018.

[18] H. Guo, H. He, and X. Xiao, "A predictive distribution model for cooperative braking system of an electric vehicle," *Mathematical Problems in Engineering*, vol. 2014, Article ID 828269, 11 pages, 2014.

[19] Y. Lu, L. Tong, Y. Chen et al., "Study of regenerative braking strategy for electric vehicle based on fuzzy logic control," *China Science Paper*, vol. 12, no. 4, pp. 398–402, 2017.

[20] J. W. Ko, S. Y. Ko, I. S. Kim, D. Y. Hyun, and H. S. Kim, "Cooperative control for regenerative braking and friction braking to increase energy recovery without wheel lock," *International Journal of Automotive Technology*, vol. 15, no. 2, pp. 253–262, 2014.

[21] G. Li and Z. Yang, "Energy saving control based on motor efficiency map for electric vehicles with four-wheel independently driven in-wheel motors," *Advances in Mechanical Engineering*, vol. 10, no. 8, pp. 64–82, 2018.

[22] E. Xing, P. Wang, X. Shang et al., "Regenerative braking technology for electric vehicle," *Science Technology and Engineering*, vol. 18, no. 25, pp. 116–127, 2018.

[23] J. Brady and M. O'Mahony, "Development of a driving cycle to evaluate the energy economy of electric vehicles in urban areas," *Applied Energy*, vol. 177, no. 5, pp. 165–178, 2016.

[24] S. Zhang and X. T. Zhuan, "Study on adaptive cruise control strategy for battery electric vehicle," *Mathematical Problems in Engineering*, vol. 2019, Article ID 7971594, 14 pages, 2019.

[25] L. Yao, L. Chu, F. Zhou, M.-H. Liu, Y.-S. Zhang, and W.-R. Wei, "Simulation and analysis of potential of energy-saving from braking energy recovery of electric vehicle," *Journal of Jilin University*, vol. 43, no. 1, pp. 6–11, 2013.

[26] Y. Xiong, Q. Yu, S. Yan et al., "Research on the influence of working conditions characteristic parameters on energy consumption for plug-in hybrid electric vehicle," *Automobile Technology*, vol. 12, no. 12, pp. 23–28, 2019.

[27] J. Wu, C. Zhang, and N. Cui, "Fuzzy energy management strategy for a hybrid electric vehicle based on driving cycle recognition," *International Journal of Automotive Technology*, vol. 13, no. 7, pp. 1159–1167, 2012.

[28] R. Günther, T. Wenzel, M. Wegner, and R. Rettig, "Big data driven dynamic driving cycle development for busses in urban public transportation," *Transportation Research Part D: Transport and Environment*, vol. 51, no. 5, pp. 276–289, 2017.

[29] B. Lorenzo, D. Massimo, and P. Marco, "Development of driving cycles for electric vehicles in the context of the city of Florence," *Transportation Research Part D: Transport and Environment*, vol. 47, no. 3, pp. 299–322, 2016.

[30] L. Yang, Y. Hu, and B. Yan, "Optimal charge depleting control of plug-in hybrid electric vehicles based on driving condition," *Automotive Safety and Energy*, vol. 8, no. 1, pp. 87–96, 2017.

[31] B. Zhou, C. Tian, Y. Song, and X. Wu, "Control strategy of AFS based on estimation of tire-road friction coefficient," *Journal of Hunan University Natural Sciences*, vol. 44, no. 4, pp. 16–23, 2017.

[32] V. H. Johnson, "Battery performance models in ADVISOR," *Journal of Power Sources*, vol. 110, no. 2, pp. 321–329, 2002.